

Spin stripes in nanotubes

Alex Kleiner

*Institute of Theoretical Physics
Chalmers University of Technology and Göteborg University
S-412 96 Göteborg, Sweden*

It is shown here that electrons on the surface of a nanotube in a perpendicular magnetic field undergo spin-chirality separation along the circumference. Stripes of spin-polarization propagate along the tube, with a spatial pattern that can be modulated by the electron filling.

The emerging field of spintronics opens a new paradigm of electronics based on the electron's spin rather than charge [1]. The realization of a spin circuit requires the generation, conduction and manipulation of spin currents. Recently, a spatial control of spin currents was demonstrated by engineering a material with a spatially varying g-factor [2]. An alternative route would require a magnetic field with spatial variation on the nanometer scale. Strong variations of the field can be achieved along the circumference of a nanotube subjected to a uniform magnetic field, directed perpendicular to its axis. Here I suggest that a two dimensional electron gas (2DEG) rolled-up to a nanotube, may form spin-stripes propagating in alternating directions, as a function of the filling. This applies to the conduction electrons in fields satisfying $l \lesssim R$, where l is the Landau length $\sqrt{\hbar/|eB|}$ and R is the tube radius. At magnetic fields of $B \lesssim 10$ T for example, the radius should be $R \gtrsim 8$ nm. Such sizes frequently occur in

multi-wall carbon nanotubes (MWCNT) and in the new class of recently produced rolled-up heterostructures [3] [4]. The former, showed magneto-conductance fluctuations [5] [6], with varying interpretations in connection to the diffusive [7] or ballistic [8] [9] nature of the MWCNT charge conductance. The spin conductance of a MWCNT however, was shown to be ballistic [10] over fairly large distances ($\gtrsim 130$ nm). On the other hand, the cylindrical heterostructures, made of silicon, silicon-germanium [4] or indium-gallium and indium-arsenic [3] have the advantage of controlled radiiuses that can easily satisfy $l \lesssim R$, they can be made clean and without the problem of unknown chirality and inter-shell coupling. It was found numerically [11] that a cylindrical spinless two dimensional electron gas (2DEG) under a perpendicular magnetic field, forms Landau level like states at the top and bottom and chiral states, similar to the edge states in the Hall bar, at the sides.

The magnetic field B is taken here to be perpendicular to the surface at the lines $x = 0$ and $x = \pi R$ hereafter the north and south 'poles'. The 'equators' are at $x = \pi R/2$ and $x = 3\pi R/2$, and states located anywhere above or bellow the equators are called here 'north' or 'south' states. The vector potential on the surface of the

tube is then $\vec{A} = (0, RB \sin \frac{x}{R})$, where (x, y) are the circumferential and axis directions of the tube, respectively. The Hamiltonian of a cylindrical 2DEG in this field is,

$$H = -\frac{\hbar^2 \partial_x^2}{2m^*} + \frac{\hbar^2}{2m^*} \left(-i\partial_y + \frac{eRB}{\hbar} \sin \frac{x}{R} \right)^2 + \mu g \mathbf{s} \cdot \mathbf{B} \quad (1)$$

where m^* is the effective mass, μ is the Bohr magneton, g is the gyro-magnetic factor and \mathbf{s} is the spin operator. The longitudinal wave vector and spin are conserved since the Hamiltonian (1) does not contain the y coordinate nor other spin operators and so the operators are replaced by their eigenvalues K_y and $\pm g\mu B/2$. The wave functions for the spin-up and spin-down particles are now $\psi_{\uparrow,\downarrow} = e^{iK_y y} \chi_{\uparrow,\downarrow}(x)$. In units of $E_L/2$, where $E_L = eB\hbar/m^*$ is the Landau level energy spacing, eq. (1) becomes the following one dimensional Hamiltonian,

$$H = -l^2 \partial_x^2 + \left(K_y l + \frac{R}{l} \sin \frac{x}{R} \right)^2 \pm \frac{gm^*}{2m_e} \quad (2)$$

The Hamiltonian (2) is a variant of Hill's equation and can be easily diagonalized numerically [11]. We want to work in the regime where all the wave-functions are confined in the circumferential direction. The weakest confining potential in (2) is for $K_y = 0$, which is a double-well with minima at the poles. This potential gives, to a linear order in x , Landau levels centered at the poles, with a spatial extension of $l\sqrt{2n+1}$, where $n = 0, 1, 2 \dots$. Thus, the potential is always confining if $R \gtrsim l\sqrt{2n+1}$. The typical energy spectrum and probability distribution in this regime are shown in fig. (1).

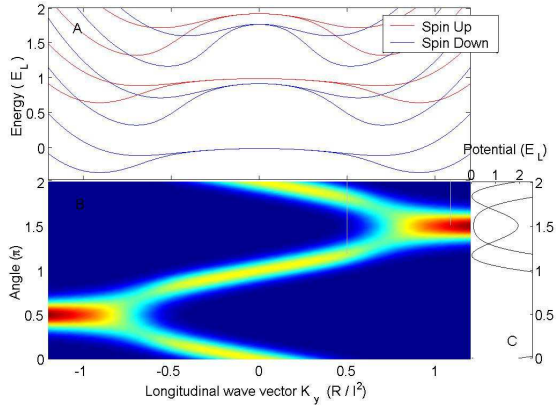


FIG. 1. Energy - Probability density phase space. (A): Energy spectrum of eq. (2), calculated numerically for $R = 2.75l$ ($R = 50\text{nm}$ and $B = 2\text{T}$), $m^* = m_e$ and $g = 2$. (B): Spatial probability distribution along the circumferential coordinate of the lowest band ($n = 0$) states in the spectrum. Here the electrons are well confined to the proximity of their potential minima. At $K_y = 0$ the potential in (2) is a double-well, one at each pole. As $|K_y|$ increases, the two wells move closer towards one of the equators, and when $|K_y| \geq R/l^2$ they merge to one well, at the equator. This point is illustrated in (C) where we zoom on the potentials of two states, $K_y = 0.5R/l^2$ and $1.1R/l^2$ marked in (B) with white lines, having a double-well and a single well potentials, respectively.

The eigenfunctions (see fig. 1B) are confined in the circumferential direction to their potential minima, depending on K_y . Since the Hamiltonian (2) is symmetric under a simultaneous sign inversion of x and K_y , states with opposite K_y are centered at opposite sides of the circumference [11], and states with $K_y = 0$ are thus centered at the poles. In the limit of a vanishing magnetic field, each band is four-fold degenerate, i.e: twice due to spin degeneracy and twice due to clock-wise and counter clock-wise propagating modes. The magnetic field removes the four degeneracies, as shown in fig. (1A), except at $K_y \approx 0$, where a two-fold degeneracy remains. Higher magnetic fields will not remove this degeneracy but rather increase it, since here, in the confinement regime, the potential for $K_y \approx 0$ has two deep and isolated potential wells at the two poles. Only as $K_y \rightarrow R/l^2$ the two potential wells get close to each other across one of the equators for their corresponding states to mix and remove the degeneracy. The total energy can be approximated analytically (see note [12]) for small K_y 's to give

$$E = \hbar\omega(n + \frac{1}{2}) + 3\lambda \left(\frac{\hbar}{2m\omega} \right)^2 (2n^2 + 2n + 1) \pm \Delta E_n + 2s \quad (3)$$

where ω , λ and ΔE_n are functions of K_y , given in the note [12] and $m \equiv m_e$, having set for simplicity $m_e = m^*$ and

$g = 2$ in Eq. (2). The first two terms in Eq. (3) are the energies of a harmonic oscillator with an anharmonic correction of a single-well potential $V(K_y)$ at a minima of Eq. (2). Since Eq. (2) has two minimas for $|K_y| < R/l^2$, these terms alone would give a two-fold degeneracy, without counting the spin. The third term largely removes this degeneracy by mixing the north and south states, and the last term is the Zeeman splitting, with $s = \pm \frac{1}{2}$. Since the conduction properties are determined only by electrons at the Fermi-energy, having the map between the energy-momentum-spin state and the spatial distribution of that state (fig. 1), we can now find the spatial distribution of the conduction electrons and their spins. The spin polarization density at a given Fermi-energy E is defined as

$P(E, x) = (P_\uparrow(E, x) - P_\downarrow(E, x)) / (P_\uparrow(E, x) + P_\downarrow(E, x))$, where the spin-up or spin-down polarization $P_{\uparrow, \downarrow}(E, x) = \sum_{K_y} g(E, K_y) |\chi_{\uparrow, \downarrow}(E, K_y, x)|^2$ factors the probability densities with the corresponding density-of-states, summed over all states K_y at the energy E . Fig. (2) shows the energy dependent spatial spin-polarization. It is dominated by states at energies with a divergent density of states $g(E) = \left(\frac{dE}{dK_y} \right)^{-1}$ at some proximity. As evident from fig. (1), these are either the Landau-like states at the poles having $K_y = 0$, or states centered around the equators, to be referred to as pole and equator singularities, respectively.

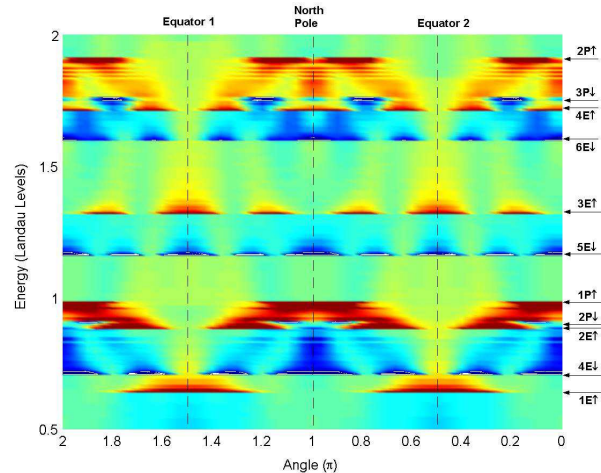


FIG. 2. Spin polarization distribution along the circumference vs. energy, with parameters as in fig. (1). The pronounced polarization densities are mainly at energies in the proximity of singularities in the density-of-states of either spin-up or spin-down bands (red and blue, respectively). Each singular spin state is either centered at a pole or around an equator. It is marked on the right with P or E respectively. e.g: the arrow labeled $1P\uparrow$ marks a singular state in the *first* sub-band, centered at the *Pole* having a spin-up.

We can follow, for example, the spatial distribution of the equator singular states carrying spin-up. There are

four such states in fig. (2), marked at the right as $1E \uparrow$ to $4E \uparrow$, where the corresponding wave-functions around each equator have, one to four peaks, respectively. A similar observation can be made for the pole singularities (marked with P in fig. 2), which are the Landau-like states. Their energy can be found analytically by simply setting $K_y = 0$ in Eq. (3), giving

$$E_n = E_L(n + \frac{1}{2} \pm \frac{1}{2}) - E_R(2n^2 + 2n + 1), \quad (4)$$

where the first term is the usual Zeeman split Landau levels and the second term is the curvature correction due to the lateral energy, $E_R = \frac{\hbar^2}{8mR^2}$. The spin-polarization $P(E, x)$ is dominated by the spin of the singular state with the closest energy to E . However, when the Fermi energy lies between the energies of singular states with opposite spins, such as between $2E \uparrow$ and $2P \downarrow$, or between $4E \uparrow$ and $3P \downarrow$ in fig. (2), there is a coexistence of spin-up and spin-down with different spatial distributions. This gives rise to the formation of spin-polarized stripes on the surface of the tube. Fig. (3) shows the spin stripes at that energy, with the additional information on the chirality of these stripes.

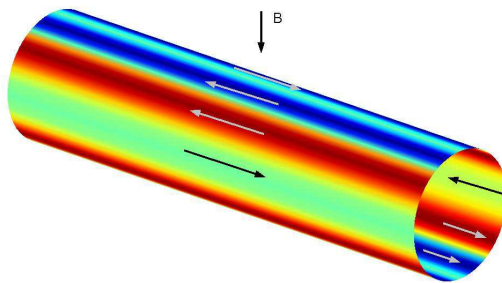


FIG. 3. Spin and chirality polarization. The Fermi-energy lies between the $2E \uparrow$ and the $2P \downarrow$ singularities in fig. (2). Red and blue colors represent, as in fig. (2), spin-up and spin-down polarizations, respectively. The arrows give the direction of propagation (chirality), taken from the sign of $\frac{dE}{dK_y}$. The black or white color of some arrows is for visibility.

There is a rather complex pattern of left moving and right moving spin ‘lanes’. The fact that spin distribution of the highest occupied electron states is entirely dependent on the filling, as shown in the polarization map (fig. 2) suggests that a gate voltage may control the spatial distribution of spins. Experimentally, it appears feasible to observe the spin-stripes spatial structure by a spin-polarized STM (SP-STM) [13], at temperatures $kT \ll E_L$. The vertical structure of the polarization

map (fig. 2) may be observed by sweeping the gate voltage with the conventional two or four point contact set-up. For short tubes, K_y in fig. (1) becomes discreet, with most of the allowed states fall at energies where the density-of-states diverges. In other words, the polarization map will converge to the discreet levels marked by the arrows on the right in fig. 2. Only one third of these levels, the pole states (eq. 4) can be considered as modified levels of the ‘flat’ quantum dot. The other levels are intrinsic to the tube. This could be supported by the experimental observation [14] that the spin dependent energy levels of a short carbon nanotube ‘dot’, do not follow the simple, flat, quantum dot level filling. However, the filling pattern in [14] can not be expected to follow the polarization map (fig. 2) since it was not conducted in the confinement regime so that other reasons, such as electron-electron interactions, may have played a more important role, as suggested by the authors. The confinement condition for the experimental resolution of spin-stripes requires either large fields or large radii. e.g: if the radius is in the range $5\text{nm} < R < 25\text{nm}$, at the lowest filling $n = 0$, the confinement condition $R \gtrsim l\sqrt{2n+1}$ gives $B \gtrsim 20\text{T}$ and $B \gtrsim 1\text{T}$, where the higher field corresponds to the lower radius. These conditions, as already noted, can be easier achieved using the cylindrical heterostructures.

In conclusion, it was shown that when a nanotube is subjected to a perpendicular magnetic field, under the specified conditions, there is a formation of spin-stripes on the surface of the tube with different propagation directions. The sensitivity of the spin pattern to the filling energy opens a potentially new way to generate and manipulate spin currents with a gate. Finally, the stripe formation may be tested directly by the recently demonstrated [13] spin-polarized scanning tunneling microscope (SP-STM).

- [1] S. A. Wolf et al., *Science* **294**, 1488 (2001)
- [2] G. Sallis et al., *Nature* **414**, 619 (2001)
- [3] V. Ya. Prinz et al. *Physica E* **6**, 828 (2000)
- [4] Oliver G. Schmidt, Karl Eberl, *Nature* **410**, 168 (2001)
- [5] C. Schönenberger et al. *Appl. Phys. A* **69**, 283 (1999)
- [6] J. O. Lee et al. *Phys. Rev. B* **61**, R16362 (2000)
- [7] C. Schönenberger and A. Bachtold, *Phys. Rev. B* **64**, 157401 (2001)
- [8] J. Kim et al., *Phys. Rev. B* **64**, 157402 (2001)
- [9] S. Roche and R. Saito, *Phys. Rev. Lett.* **87**, 246803 (2001)
- [10] K. Tsukagoshi, B. W. Alphenaar and H. Ago, *Nature* **401**, 572 (1999).
- [11] H. Ajiki and T. Ando, *J. Phys. Soc. Jpn.* **62**, 1255 (1993)
- [12] For $R \gtrsim l\sqrt{2n+1}$ all states are confined to the proximity of their potential minima, which are at $x_{min} =$

$R \sin^{-1} \frac{|K_y|l^2}{R}$ and $\pi R - x_{min}$ for $-R/l^2 \leq K_y \leq 0$, and for states with $0 \leq K_y \leq R/l^2$ at $2\pi R - x_{min}$ and $\pi R + x_{min}$. The potential at a small distance ϵ from the minima can be expanded as $V(K_y, \epsilon) = \frac{1}{2}m\omega^2\epsilon^2 + \lambda\epsilon^4$, with $\omega = \frac{1}{R}\sqrt{\frac{E_l}{m}(\frac{R^2}{l^2} - K_y^2 l^2)}$ and $\lambda = \frac{E_l}{24R^4} \left(7K_y^2 l^2 - 4\frac{R^2}{l^2}\right)$. The potential at $|K_y| \leq R/l^2$ is a double-well, symmetric about the equator, described by $V(K_y, \epsilon)$ at the vicinity of its two minima x_{min} and $\pi R - x_{min}$. Denoting $\psi_{1/2}$ for the two single well wave functions, the total wave function of state K_y , to a zeroth order is $\Psi_{s/a} = \frac{1}{\sqrt{2}}(\psi_1 \pm \psi_2)$, where s/a corresponds to the symmetric and antisymmetric product respectively. Due to the non-zero tunneling probability across the equator, the degeneracy of the symmetric and antisymmetric states is lifted. In the semi-classical approximation, the energy is split by $\frac{4\hbar^2}{m}\psi(x_{eq})\psi'(x_{eq})$ where $\psi(x_{eq})$ and $\psi'(x_{eq})$ are either one of the single well wave functions and their derivative, at the equator. Taking $\psi(x_{eq})$ to be the eigenfunctions of the harmonic part of the energy, the first two energy splittings are $\Delta E_1 = \frac{2\hbar^2}{m} \frac{1}{\sqrt{\pi a^3}} b e^{-(b/a)^2}$ and $\Delta E_2 = \frac{4\hbar^2}{m} \frac{1}{\sqrt{\pi a^5}} b^3 e^{-(b/a)^2}$, where $a \equiv \sqrt{\frac{\hbar}{m\omega}}$ and $b = R(\pi/2 - \sin^{-1} \frac{K_y l^2}{R})$. This result agrees with the numerics for $|K_y| \lesssim \frac{R}{2l^2}$.

- [13] Heinze S. et al., *Science* 288, 1805 (2000)
- [14] Sander J. Tans et al., *Nature* 394, 761 (1998)

ACKNOWLEDGMENTS

I am indebted to Sebastian Eggert for many discussions and to Kim Jaeuk, Mikael Fogelström and Paata Kakashvili for helpful comments on the manuscript.